

## **Distribution Agreement**

In presenting this thesis as a partial fulfillment of the requirements for a degree from Emory University, I hereby grant to Emory University and its agents the non-exclusive license to archive, make accessible, and display my thesis in whole or in part in all forms of media, now or hereafter now, including display on the World Wide Web. I understand that I may select some access restrictions as part of the online submission of this thesis. I retain all ownership rights to the copyright of the thesis. I also retain the right to use in future works (such as articles or books) all or part of this thesis.

Patan Tippitak

April 1, 2024

Synergistic Paradigm of Radiotherapy and PD-L1 Blockade Orchestrates the Induction of Stem-Like T Cell Populations within the Tumor-Draining Lymph Node

by

Patan Tippitak

Zachary S. Buchwald MD PhD

Adviser

Chemistry

Zachary S. Buchwald MD PhD

Adviser

Cora E. MacBeth PhD

Committee Member

Richard A. Himes PhD

Committee Member

2024

Synergistic Paradigm of Radiotherapy and PD-L1 Blockade Orchestrates the Induction of Stem-Like T Cell Populations within the Tumor-Draining Lymph Node

By

Patan Tippitak

Zachary S. Buchwald MD PhD

Adviser

An abstract of  
a thesis submitted to the Faculty of Emory College of Arts and Sciences  
of Emory University in partial fulfillment  
of the requirements of the degree of  
Bachelor of Science with Honors

Chemistry

2024

## Abstract

### Synergistic Paradigm of Radiotherapy and PD-L1 Blockade Orchestrates the Induction of Stem-Like T Cell Populations within the Tumor-Draining Lymph Node

By Patan Tippitak

Combined Radiotherapy (RT) and anti-PD-L1 therapies are known to augment control of both local and distant (abscopal) tumors. Variability exists in human clinical responses, however, which necessitates a deeper exploration of the cooperative mechanisms involved. This investigation targets the synergistic interactions between RT and anti-PD-L1 at the cellular level, specifically focusing on the role of a CD8<sup>+</sup> PD-1<sup>+</sup> Tcf-1<sup>+</sup> stem-like T cell population within the tumor-draining lymph node (TdLN). Experimental designs employing melanoma murine models have revealed that simultaneous administration of RT and anti-PD-L1 orchestrates a unique program of differentiation within TdLN stem-like T cells. This program catalyzes their expansion and differentiation into intratumoral effector cells within the tumor microenvironment. Our data also suggest that the enhanced antitumor efficacy arising from the combination of RT and anti-PD-L1 critically hinges on the integrity and functionality of the stem-like T cell population in the TdLN. Impediments to the migratory egress of these cells from the TdLN or the targeted depletion of this specific subset attenuate the therapeutic efficacy. This study elucidates a complex, phased induction process of stem-like T cells beginning within the TdLN and reaching completion within the tumor microenvironment, fundamental to the combined treatment's effectiveness.

Synergistic Paradigm of Radiotherapy and PD-L1 Blockade Orchestrates the Induction of Stem-Like T Cell Populations within the Tumor-Draining Lymph Node

By

Patan Tippitak

Zachary S. Buchwald MD PhD

Adviser

A thesis submitted to the Faculty of Emory College of Arts and Sciences  
of Emory University in partial fulfillment  
of the requirements of the degree of  
Bachelor of Science with Honors

Chemistry

2024

## Table of Contents

<b>Background Information</b>	1
<b>Results and Figures</b>	4
<i>Figure 1.</i> Combining RT and anti-PD-L1 Therapy Elevates Intra-tumoral Stem-Like and Terminal Effector CD8+ T Cell Populations	5
<i>Figure 2.</i> TdLN Serves as a Reservoir of Stem-Like CD8+ T Cells and Supplies the Tumor After RT + Anti-PD-L1 Therapy	7
<i>Figure 3.</i> RT and Anti-PD-L1 Therapy Reprogram CD8+ T-cell Gene Expression Profiles in the TdLN	9
<i>Figure 4.</i> RT Enhances the Expansion and Differentiation of TdLN Stem-Like T Cells, Further Augmented by Anti-PD-L1	10
<b>Discussion</b>	12
<b>Methods</b>	14
<b>References</b>	17
Supporting Figures	20

## **Background Information**

CD8+ T cells are pivotal in orchestrating the immune system's defense against cancer, employing a variety of mechanisms to identify and eliminate tumor cells. Their efficacy, however, is not without limitation, particularly in the context of chronic antigen exposure characteristic of cancerous environments. Such conditions induce a state known as CD8+ T cell exhaustion, a phenomenon characterized by diminished effector functions, proliferative capacity, and the upregulation of inhibitory receptors such as PD-1 and Tim3.<sup>1-3</sup> This state is further compounded by epigenetic modifications that alter gene expression profiles, contributing to the impaired functionality of these cells within the tumor microenvironment.<sup>1-3</sup>

The intervention with PD-1 blockade therapies represents a significant advance, aiming to reverse this exhaustion by blocking inhibitory signals, thereby promoting the expansion and reinvigoration of CD8+ T cells. This approach has yielded impressive clinical outcomes across a spectrum of cancers, underscoring the potential of immunotherapy as a cornerstone of cancer treatment.<sup>4-7</sup> Within the tumor microenvironment, CD8+ PD-1+ T cells exhibit remarkable heterogeneity, comprising both progenitor stem-like cells and terminally differentiated effector-like cells (TE).<sup>8,9</sup> The former, characterized by the expression of the transcription factor Tcf-1, retains a capacity for proliferation and differentiation into effector cells capable of expressing granzyme B, a critical molecule for the cytolytic activity against tumor cells.<sup>10,11</sup>

Despite the successes of PD-1 blockade therapy, its efficacy is not universal, achieving durable tumor control in only a subset of patients. This variability in response has catalyzed interest in developing combinatorial therapeutic strategies. By integrating PD-1 blockade with other treatments, there is potential to not only amplify the reactivation of exhausted CD8+ T cells but also to harness the full spectrum of immune mechanisms against tumor cells. Such combinatorial approaches are grounded on a nuanced understanding of the tumor immune environment, T cell physiology, and the intricate mechanisms of immune evasion employed by cancer cells. Therefore, exploring these synergistic treatments opens avenues for significantly improved patient outcomes and the realization of the full promise of cancer immunotherapy.

Radiotherapy (RT), a cornerstone in the arsenal against cancer, serves not only as a powerful local treatment modality but also wields significant immunomodulatory capabilities. Beyond its direct cytotoxic impact on tumor cells, RT facilitates a broader immune response, at times inducing tumor regression beyond the confines of the irradiated area. This phenomenon, known as the abscopal effect<sup>12-14</sup>, represents a paradigm shift in understanding the systemic implications of localized treatments. The abscopal effect, though clinically infrequent, underscores the potential of RT to function analogously to an in-situ vaccine. By causing tumor cell death, RT releases a multitude of tumor antigens, simultaneously broadening the T cell receptor repertoire and mobilizing naïve and antigen-experienced T cells into the anti-tumor immune response. This expansion and recruitment of T cells are pivotal for enhancing the organism's ability to recognize and combat tumor cells dispersed throughout the body.

The potential for RT to synergize with immune checkpoint blockade therapies, such as those targeting the PD-1/PD-L1 interaction, has garnered substantial interest.<sup>15-18</sup> This combination has been postulated to capitalize on the strengths of both modalities: RT's ability to expose and present tumor antigens, and checkpoint blockade's capacity to alleviate the brakes on the immune system, potentially overcoming T cell exhaustion and revitalizing the anti-tumor immune response. Preliminary clinical findings suggest this approach holds considerable promise<sup>18,19</sup>, indicating a potentiation of therapeutic effects beyond what either modality can achieve independently. Despite these advancements, the complexity of the immune response to cancer, coupled with the variability in individual patient outcomes, necessitates the critical need for a deeper, mechanistic understanding of how RT and checkpoint blockade interact. Particularly pressing is the need to elucidate how RT influences T cell dynamics, potentially reversing exhaustion and fostering a more robust and durable immune response. As such, investigating the synergistic potential of combined RT and PD-1/L1 blockade not only offers insights into enhancing treatment efficacy but also into tailoring therapies to leverage the immune system's full anti-tumor potential.

The tumor-draining lymph node (TdLN) plays a pivotal role in fostering a robust immune response triggered by RT or anti-PD-1/L1 therapy.<sup>20-24</sup> Emerging research has shed light on the significance of the TdLN as a reservoir for a distinct population of stem-like T cells<sup>22,25,26</sup>, a discovery that has profound implications for immunotherapeutic strategies. This population of stem-like T cells within the TdLN serves as developmental precursors for the intra-tumoral T cell population, continuously migrating from the TdLN to the tumor microenvironment under normal physiological conditions.<sup>25</sup> Once these stem-like T cells infiltrate the tumor, they undergo further differentiation into TE, enhancing the immune response within the tumor microenvironment. Studies by Huang et al. have illustrated the critical role of the TdLN stem-like population in mediating the efficacy of anti-PD-1/L1 therapy<sup>22</sup>, emphasizing its significance in shaping the therapeutic response. Building upon these insights, previous research, including our own, has suggested that the reservoir of stem-like T cells in the TdLN may also contribute to the immune response stimulated solely by RT.<sup>21</sup> This collective body of evidence underscores the central role of the TdLN stem-like T cell population in driving the synergistic effect observed between radiotherapy and anti-PD-L1 therapy, highlighting its potential as a target for therapeutic intervention aimed at bolstering immunotherapy outcomes.

In this study, we explore the effects of RT alone and in combination with PD-L1 blockade on the behavior and fate of stem-like T cells within the TdLN using murine models of melanoma. Our investigations reveal that the combined application of RT and PD-L1 blockade elicits a marked enhancement in the differentiation processes of these stem-like T cells within the TdLN. This enhancement is mediated through the activation of a previously uncharacterized transcriptional program, which not only prompts the initial differentiation of these stem-like T cells but also induces their substantial proliferation. Following this programmatic shift, the stem-like T cells



transition into TE, a transformation that continues as they migrate into and infiltrate the tumor microenvironment.

Our findings illuminate the significant impact that this enhanced differentiation and subsequent effector function have on tumor control. Notably, the efficacy of this combination therapy in controlling both primary (local) and metastatic (distant) tumor sites is intricately tied to the presence and functional integrity of the stem-like T cell population within the TdLN.

Furthermore, the migratory egress of these newly differentiated effector cells from the TdLN to the tumor plays a pivotal role in mediating the observed therapeutic benefits. These observations collectively underscore the integral role of the TdLN's stem-like T cell subset in mediating the enhanced antitumor immunity elicited by the combined application of RT and PD-L1 blockade.

Through detailed molecular and cellular analyses, this research investigation provides a deeper understanding of how combined therapeutic strategies can be leveraged to reinvigorate the immune system's natural capacity to combat cancer. By outlining the pathway through which stem-like T cells in the TdLN are activated, proliferate, and differentiate in response to these therapies, we offer novel insights into the mechanistic underpinnings of effective cancer immunotherapy strategies. This knowledge not only advances our comprehension of the dynamic interplay between therapeutic interventions and immune responses but also sets the stage for the development of more targeted and efficacious treatment paradigms designed to harness the immune system's full anti-cancer potential.

## **Results and Figures**

### **Combining RT and anti-PD-L1 Therapy Elevates Intra-tumoral Stem-Like and Terminal Effector CD8+ T Cell Populations**

In our prior investigation, it was demonstrated that radiotherapy (RT) alone could augment the anti-tumor immune response, resulting in enhanced tumor suppression through a mechanism dependent on CD8+ T cells.<sup>21</sup> In the current study, we sought to explore the effects of combining RT with anti-PD-L1 therapy on both local and distal (abscopal) tumor control, as well as the dynamics of CD8+ T cell subsets. To this end, B16F10 melanoma cells engineered to express the lymphocytic choriomeningitis virus (LCMV) glycoprotein (B16F10GP) were sequentially implanted into the bilateral flanks of wild-type C57BL/6 mice (Figure 1A), facilitating the identification of tumor-specific T cells.<sup>21</sup> This approach of sequential tumor implantation was employed to simulate metachronous metastatic disease. The first tumor to be implanted (Tumor 1) received a single dose of 10 Gy RT (Figure S1A), administered either with or without anti-PD-L1 therapy, commencing on the 10th day following implantation.<sup>21</sup> Mice were euthanized 9 days post-treatment initiation (day 19) for subsequent tissue analysis (Figure 1A).

Analysis revealed that RT alone significantly curtailed the growth of both Tumor 1 and the subsequently implanted Tumor 2 (Figure 1B, S1B-S1C). In contrast, treatment with anti-PD-L1 in isolation had a minimal impact on the growth of both tumors, which aligns with the previously documented resistance of this cell line to PD-1 pathway inhibition.<sup>27,28</sup> Notably, the combined regimen of RT and anti-PD-L1 markedly impeded the progression of both the treated Tumor 1 and the untreated Tumor 2, demonstrating a superior efficacy over either treatment modality administered singly (Figure 1B, S1B-S1C). Parallel kinetic analyses conducted on both the original B16F10 cell line and another melanoma cell line (YUMM1.7) corroborated the potent synergistic effect of RT and anti-PD-L1 at both primary and abscopal sites (Figure S1D).

Subsequently, our examination focused on the anti-tumor immune response, particularly regarding the population of bulk CD8+ T cells within both tumors. It was observed that neither RT nor anti-PD-L1 therapy, when applied independently, resulted in a notable augmentation of CD8+ T cell counts in either tumor. Conversely, the combined application of these therapies significantly enhanced the presence of CD8+ T cells in both tumors (Figure S1E). Further analysis of tumor-specific CD8+ Gp33+ T cells revealed a considerable elevation in their numbers in both tumors following the combination therapy, as opposed to either no treatment or monotherapy (Figure 1C–1D).

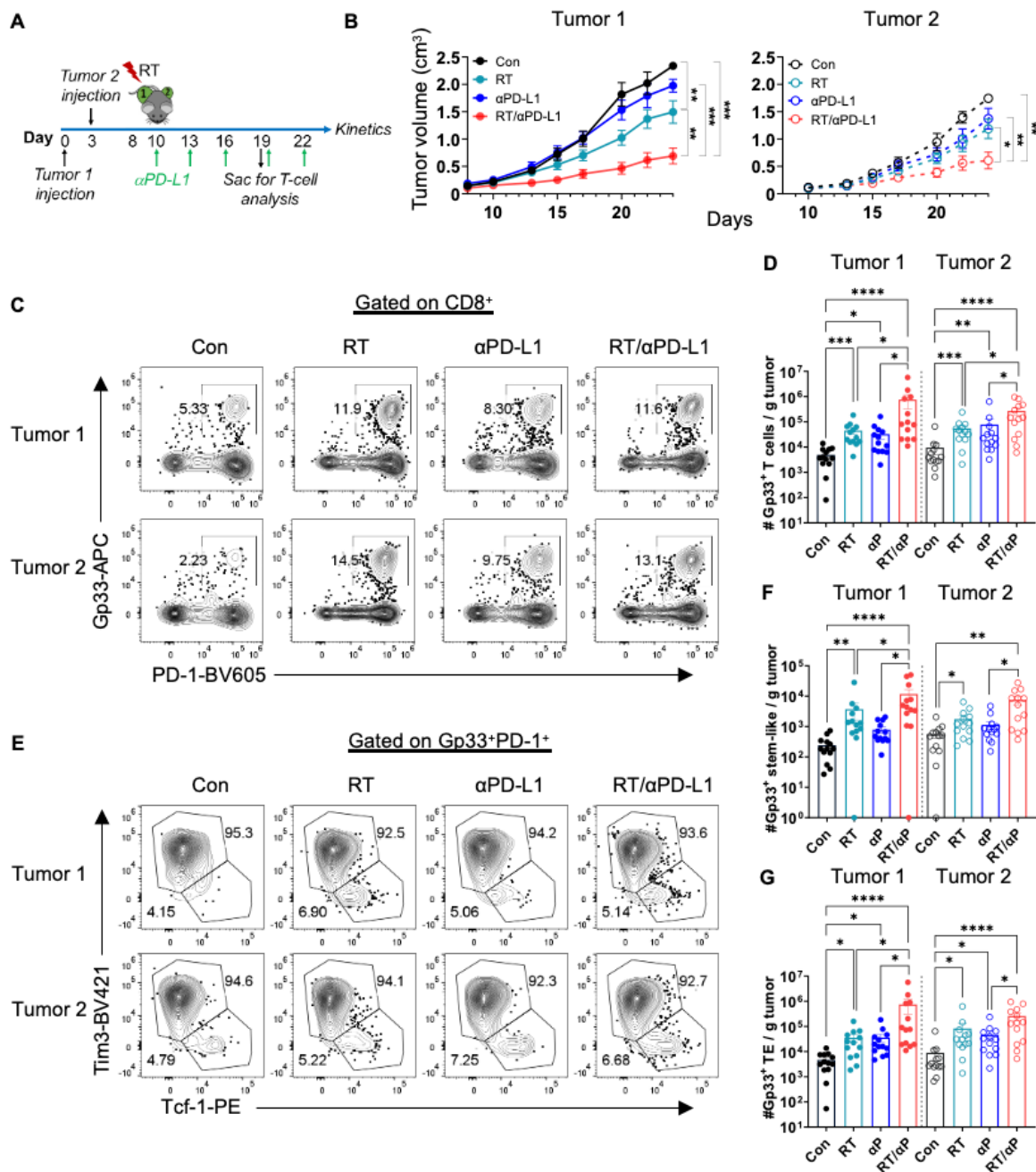


**Figure 1. Combining RT and anti-PD-L1 Therapy Elevates Intra-tumoral Stem-Like and Terminal Effector CD8+ T Cell Populations.** (A) Experiment design. (B) Kinetics of tumor growth in both the irradiated tumor (Tumor I) and non-irradiated (abscopal) tumor (Tumor 2), showing improved suppression with the use of combination therapy. Results aggregate data from two distinct experiments (n=10 in total). (C) Flow cytometry plots of Gp33+ PD-1+ T cells gated on CD8+ populations in Tumor 1 and Tumor 2 across various treatment conditions. (D) Quantitative illustration of Gp33+ T cell count per gram of tumor tissue. (E) Flow cytometry plots of Tim3–Tcf-1+ stem-like T cells and Tim3+ Tcf-1– TE T cells, both subsets gated on CD8+ PD-1+ Gp33+ T cells. (F) Quantitative illustration of stem-like T cell count per gram of tumor tissue. (G) Quantitative illustration of TE T cell count per gram of tumor tissue. Significance levels indicated as follows: \*p<0.05, \*\*p<0.01, \*\*\*p<0.001, \*\*\*\*p<0.0001, determined by ANOVA. Data combine results from three independent experiments (n = 13 total).

Of particular interest, within the subset of tumor-specific CD8<sup>+</sup> Gp33<sup>+</sup> T cells, both the stem-like and TE subsets experienced significant growth in tumors 1 and 2 subsequent to the combined RT and anti-PD-L1 therapy. Noteworthy was the observation that the relative proportions of these subsets remained unchanged (Figure 1E–1G, S1F-G).

Completing this segment of the analysis, the functionality of CD8<sup>+</sup> T cells post-combination therapy was evaluated. This involved restimulating bulk tumor CD8<sup>+</sup> T cells *ex vivo* with the Gp33 peptide. The findings indicated that monotherapies involving RT or anti-PD-L1 did not significantly influence either the frequency or the abundance of IFN- $\gamma$ <sup>+</sup> and IFN- $\gamma$ <sup>+</sup> TNF- $\alpha$ <sup>+</sup> T cells. In stark contrast, the combination therapy precipitated significant increases in both parameters (Figures S1H-S1K).

### **TdLN Serves as a Reservoir of Stem-Like CD8<sup>+</sup> T Cells and Supplies the Tumor After RT + Anti-PD-L1 Therapy**

Previous research has underscored the critical role of stem-like T cells in mediating the response to chronic viral infections and cancer following stimulation by anti-PD-1/L1 therapies.<sup>10,11</sup>

Furthermore, both our work and that of others have identified the TdLN as a crucial reservoir for these stem-like T cells, which are then recruited to the tumor site<sup>21,22,25,26</sup>. Specifically, tumor antigen-specific T cells are predominantly located within the TdLN, as opposed to non-TdLN or other secondary lymphoid organs like the spleen (Figure S2A). Our previous findings indicated that impairment of this reservoir through TdLN immunodepletion hindered the immunostimulatory effect of RT alone.<sup>21</sup> These observations suggest the pivotal importance of the stem-like T cell reservoir within the TdLN for the synergistic effect observed with combined RT and anti-PD-L1 therapy.

To further investigate this hypothesis, we verified that the majority of Gp33<sup>+</sup> T cells within the TdLN exhibit a stem-like phenotype (Tim3<sup>-</sup> Tcf-1<sup>+</sup>), whereas those within the tumor predominantly represent the terminal effector (TE) subset (Figure 2A–2B). Mice were then administered FTY720 before receiving RT or anti-PD-L1 treatment, a strategy designed to inhibit lymphocyte migration from the TdLN and other secondary lymphoid structures (Figure 2C). This intervention led to a significant reduction in the levels of circulating lymphocytes, including both CD4<sup>+</sup> and CD8<sup>+</sup> T cells (Figures S2B-S2D). Following combination therapy, the observed increases in total CD8<sup>+</sup> and Gp33<sup>+</sup> T cells within both tumors were hindered by FTY720 administration (Figure 2D–2E, S2E-S2G). Moreover, FTY720 treatment nullified the augmentation in tumor-antigen specific stem-like and TE subsets within the tumor, an effect previously induced by combination therapy (Figures 2F–2H, S2H-S2J). Crucially, the deceleration of tumor growth effected by the combination of RT and anti-PD-L1 was also mitigated by FTY720 (Figure 2I, S2K).

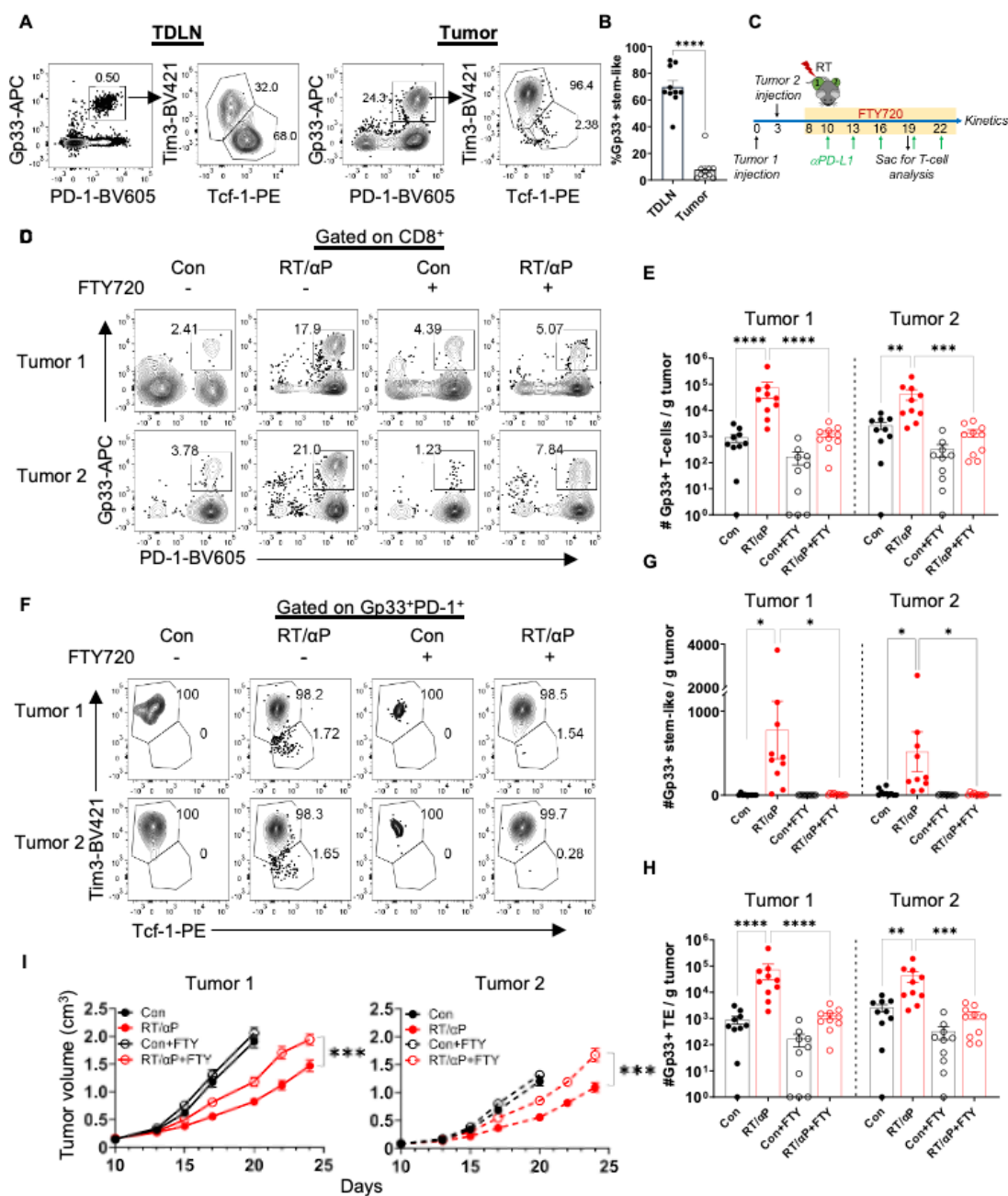


**Figure 2. TdLN Serves as a Reservoir of Stem-Like CD8+ T Cells and Supplies the Tumor After RT + Anti-PD-L1 Therapy.** (A) Flow cytometry plots of PD-1+ Gp33+ T cells, distinguishing stem-like from TE T cells in tumors and TdLN. (B) Prevalence of stem-like T cells in TdLN and tumor. (C) Experimental timeline with FTY720 administration in drinking water marked by a yellow bar. (D) Flow cytometry plots gated on CD8+ cells showing PD-1+ Gp33+ T cells in tumors, with and without FTY720. (E) Gp33+ T cell count per gram of tumor, as per conditions in subfigure D. (F) Antigen-specific T cell subsets under various treatments, with and without FTY720. (G) Antigen-specific stem-like T cell count per gram of tumor, as per conditions in subfigure F. (H) Antigen-specific TE T cell count per gram of tumor, as per conditions in subfigure F. Data combined from two experiments (n=10 each). (I) Tumor growth kinetics with and without FTY720. Significance levels are denoted as follows: \*p<0.05, \*\*p<0.01, \*\*\*p<0.001, \*\*\*\*p<0.0001, based on two-tailed t-tests. Data combine results from two experiments (n = 15 total).

In the TdLN, the administration of RT combined with anti-PD-L1 did not alter the frequency or quantity of total CD8<sup>+</sup> T cells, regardless of whether FTY720 was used (Figure S3A-S3B). However, a notable increase in the frequency of CD8<sup>+</sup> PD-1<sup>+</sup> Gp33<sup>+</sup> T cells was observed following FTY720 treatment, with the total count of PD-1<sup>+</sup> Gp33<sup>+</sup> T cells nearing statistical significance (Figure S3C-S3E). Crucially, the presence of Gp33<sup>+</sup> stem-like T cells in the TdLN saw a significant upsurge when FTY720 was combined with the therapy, highlighting the distinct response of this subset (Figures S3F-S3H); in contrast, the TE population did not exhibit a significant increase (Figure S3I-S3J).

These findings lend robust support to the hypothesis that the enhancement of tumor stem-like T cells following RT and anti-PD-L1 therapy is reliant on their migration from the TdLN. This suggests a pivotal role of lymphatic trafficking in mediating the therapeutic synergy between RT and anti-PD-L1, emphasizing the importance of the TdLN as a reservoir for immunologically competent cells capable of contributing to tumor control.

### **RT and Anti-PD-L1 Therapy Reprogram CD8<sup>+</sup> T-cell Gene Expression Profiles in the TdLN**

To discern the effect of combination therapy versus monotherapy on T cell populations within the TdLN, we conducted single-cell RNA sequencing (scRNA-seq) on sorted CD8<sup>+</sup> PD-1<sup>+</sup> T cells collected 7 days post-treatment. Treatments under review included anti-PD-L1, RT alone, and their combination. This analysis encompassed a total of 38,578 cells, averaging 1,928 cells per sample, with each treatment group consisting of 5 mice.

The annotation of unsupervised clustering identified five principal populations of CD8<sup>+</sup> T cells. Intriguingly, the gene expression profiles of CD8<sup>+</sup> T cells from untreated mice bore resemblance to those from mice treated with either anti-PD-L1 or RT alone, suggesting minimal impact of monotherapies on the transcriptional landscape of these cells. Conversely, dimensionality reduction techniques revealed marked phenotypic disparities between mice subjected to the RT + anti-PD-L1 combination therapy and those treated with either form of monotherapy.

To delve deeper into the alterations in gene expression induced by therapy, a pathway enrichment analysis was performed. This analysis focused on identifying the specific changes in gene expression within CD8<sup>+</sup> T cells attributable to combination therapy. Notably, the analysis revealed a downregulation in the expression of genes associated with inhibitory and exhaustion markers, such as *Tox*, *Ctla4*, *Dusp1*, *Dapl1*, and *Btla*, in CD8<sup>+</sup> PD-1<sup>+</sup> T cells derived from the TdLN of mice treated with the combination therapy. This was in stark contrast to the gene expression observed in CD8<sup>+</sup> T cells from untreated mice or those treated with anti-PD-L1 or RT alone (Figure 3).

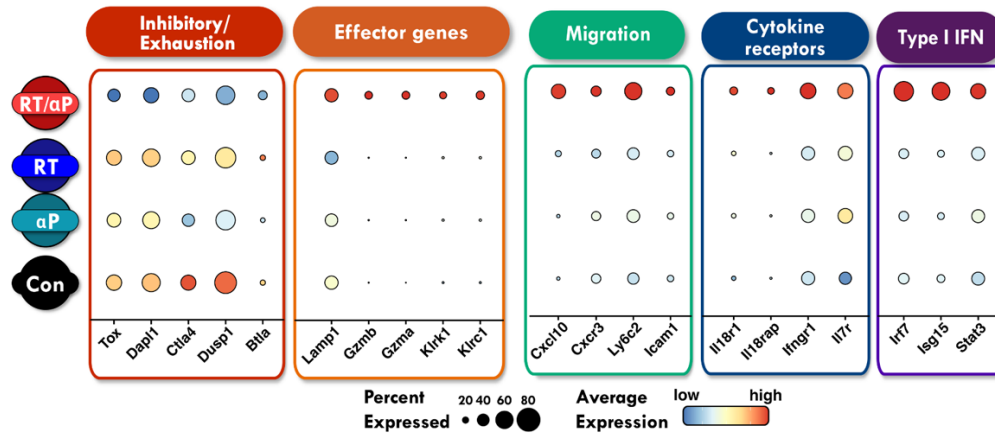


**Figure 3. RT and Anti-PD-L1 Therapy Reprogram CD8+ T-cell Gene Expression Profiles in the TdLN.** Selected gene clusters exhibited differential expression in the group receiving combination therapy.

Conversely, there was a significant upregulation in genes related to effector molecules (Gzmb, Gzma, Klrk1, Lamp1, and Tbx21), cytokine receptors (Il18r1, Il18rap, Ifngr1, and Il7r), and type I interferon signaling (Irf7, Isg15, Stat3) following combination therapy. A particularly noteworthy aspect of the gene expression changes was the enhanced expression of genes implicated in migration (Cxcl10, Cxcr3, Ly6c2, and Icam1), suggesting an augmented migratory capacity of CD8+ T cells from the TdLN post-combination therapy (Figure 3).

These findings collectively indicate that combination therapy not only reduces the expression of exhaustion-related genes in CD8+ PD-1+ T cells but also upregulates genes associated with effector functions, cytokine signaling, and cell migration. This reprogramming of CD8+ PD-1+ T cells by combination therapy fosters a phenotype characterized by increased cytotoxic and migratory capabilities, all the while preserving a stem-like phenotype. This enhanced functional profile suggests a potentiated anti-tumor immune response facilitated by the combination therapy, providing a cellular basis for its observed efficacy.

### **RT Enhances the Expansion and Differentiation of TdLN Stem-Like T Cells, Further Augmented by Anti-PD-L1**

The existing literature has highlighted that monotherapy with anti-PD-L1 fosters the proliferation and differentiation of stem-like T cells.<sup>11</sup> Our single-cell RNA sequencing (scRNA-seq) analysis suggests that, akin to monotherapy, combination therapy also supports the differentiation of stem-like T cells, while instigating a distinct transcriptional response in the TdLN. To delve deeper into these findings and ascertain the effects of RT alone and in combination with anti-PD-L1 on the differentiation of stem-like T cells, we conducted a series of adoptive transfer experiments utilizing P14 T cells.

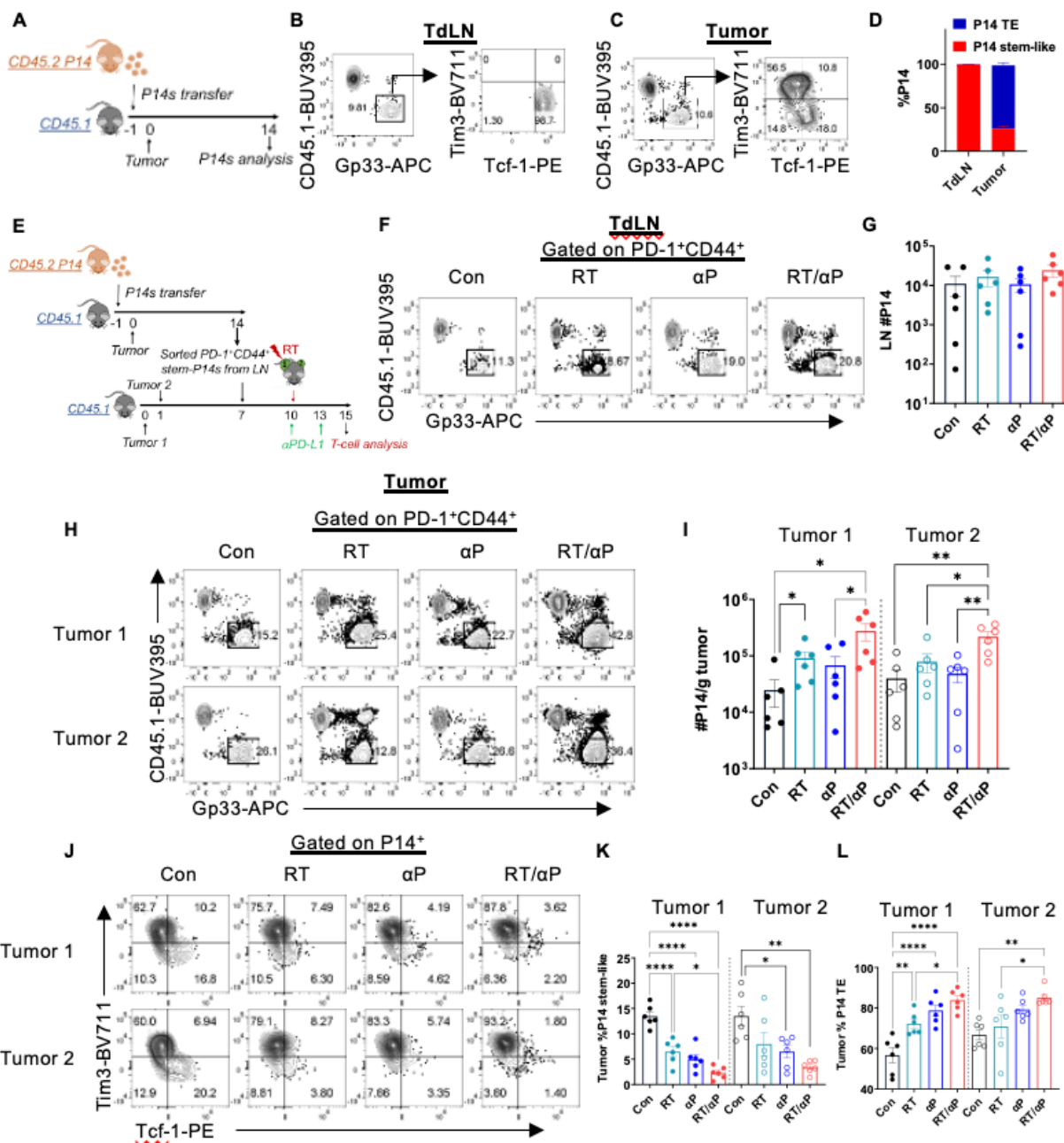


**Figure 4. RT Enhances the Expansion and Differentiation of TdLN Stem-Like T Cells, Further Augmented by Anti-PD-L1.** (A) Experimental design. (B) Flow cytometry plots illustrating stem-like P14 T cells in the TdLN. (C) Flow cytometry plots illustrating effector P14 T cells in the TdLN. (D) Comparison of stem-like and TE P14 T cell frequencies between the TdLN and tumor. (E) Experimental design featuring serial adoptive transfers. (F) Flow cytometry plots gated on transferred P14 cells in the TdLN across various treatment conditions. (G) Quantification of P14 cells in the TdLN by treatment. (H) Flow cytometry plots gated on transferred P14 cells in the tumor under different treatment conditions. (I) P14 cell count per gram of tumor. (J) Flow cytometry plots illustrating P14 T cell subsets within tumors. (K) Proportion of stem-like cells within tumors. (L) Proportion of TE cells within tumors. Significance levels indicated as follows: \* $p < 0.05$ , \*\* $p < 0.01$ , \*\*\* $p < 0.001$ , \*\*\*\* $p < 0.0001$ , determined by ANOVA. Data combine results from two independent experiments ( $n = 6$  total).



Initially, mice were euthanized 14 days post-tumor injection to verify if naïve P14 T cells could home to the TdLN and the tumor, adopting stem-like and TE phenotypes similar to endogenous cells following the first round of adoptive transfer (Figure 4A). P14 T cells were successfully recovered from both the TdLN and tumor sites, with an overwhelming majority (99%) exhibiting a stem-like phenotype in the TdLN and a TE phenotype within the tumor (Figure 4B–D).

Subsequently, CD44<sup>+</sup> PD-1<sup>+</sup> Tim3<sup>-</sup> stem-P14 cells were isolated from the TdLNs and transferred into mice bearing B16F10GP tumors. These mice were then subjected to RT with or without anti-PD-L1 treatment three days later (Figure 4E, S5A). No significant variance was noted in the counts of P14 or P14 Tcf-1<sup>+</sup> T cells in the TdLN between the monotherapy and combination therapy groups (Figure 4F–4G, S5B). Nonetheless, phenotypic alterations within the TdLN population were evident following combination therapy, consistent with our transcriptional analysis (Figure S5C–S5D). These outcomes provide concrete evidence that the unique subset of T cells exhibiting enhanced functionality arises from stem-like precursors within the TdLN, affirming the critical role of this reservoir in the differentiation process influenced by combination therapy.

Shifting focus to the tumors, our observations revealed a notable increase in the population of P14 T cells within tumor 1 following RT alone, indicating the therapy's potential to stimulate both the expansion and differentiation of TdLN-derived stem-like T cells within the targeted tumor (Figure 4H–4I). This was further evidenced by a significant reduction in the frequency of stem-like cells and a corresponding rise in the frequency of TE cells with RT treatment, demonstrating the therapy's capacity to foster the transformation of stem-like T cells into their effector counterparts (Figure 4J–4L).

Crucially, the combination of RT with anti-PD-L1 therapy resulted in a more pronounced expansion of stem-like P14 T cells in both tumor 1 and tumor 2, as compared to monotherapy. This effect was accompanied by an enhanced differentiation of stem-like T cells into TE cells, surpassing what was observed with RT alone (Figure 4H–4L). These findings collectively suggest that combination therapy triggers a unique differentiation trajectory for TdLN-resident stem-like T cells, characterized by their migration to the tumor, subsequent proliferation, and effector differentiation.

This phenomenon underscores the synergistic effect of combining RT with anti-PD-L1 therapy, not only in amplifying the presence of effector T cells within tumors but also in orchestrating a complex immunological response that begins with the reprogramming of stem-like T cells within the TdLN. The initiation of this novel differentiation program, followed by the migration and effector transformation of T cells in the tumor environment, highlights the intricate mechanisms through which combination therapy enhances anti-tumor immunity.

## **Discussion**

Our study was conducted to elucidate the mechanism behind the observed synergistic effect of radiation therapy (RT) and anti-PD-L1 treatment, focusing on a Tcf-1+ stem-like T cell subset. Employing murine melanoma models, we discovered that the combined therapy initiates a novel differentiation program within the stem-like T cells in the tumor-draining lymph nodes (TdLN). These cells, once in the tumor environment, undergo robust expansion and differentiate into terminal effector (TE) cells. We further demonstrated that the enhanced efficacy in tumor suppression through the combination of RT and anti-PD-L1 is contingent upon this specific TdLN subset. Drawing on these findings, we propose a comprehensive model involving multiple stages and tissues, starting from the TdLN and concluding within the tumor. This model carries profound implications, extending from basic biological insights to practical clinical applications.

The discovery that the combination of RT and anti-PD-L1 treatment triggers a novel differentiation program, leading to more vigorous proliferation of stem-like T cells, is striking from a biological standpoint. RT has been documented to facilitate the release of cryptic or sequestered tumor antigens, activate IFN-I signaling, and prompt the emission of damage-associated molecular patterns (DAMPs), stimulating enhanced maturation of antigen-presenting cells (APCs) and activation of T cells.<sup>30,31</sup> Notably, previous research has primarily concentrated on the intra-tumoral T cells, overlooking subsets within secondary lymphoid organs.<sup>17</sup> Our findings indicate that the antigen surge and/or cytokine production induced by RT are sufficient to initiate stem-like T cell expansion and differentiation in the TdLN. This effect is further augmented and altered in the presence of anti-PD-L1. This finding is particularly innovative since, until now, the differentiation of robust stem-like T cells was believed to be predominantly reliant on PD-1/L1 blockade. The investigation into whether APC migration from the tumor to the TdLN occurs, or if antigens passively drain to the node following RT, remains a vibrant area of research and will be the emphasis of forthcoming studies.

From a clinical perspective, our findings have broad and significant implications. Numerous clinical trials that have assessed the efficacy of combining RT with checkpoint blockade have yielded mixed to modest results.<sup>18,19,32,33</sup> Specifically, many of these trials have concentrated on treating extensive areas with elective nodal irradiation, particularly in cases of head and neck cancer.<sup>33</sup> Recent evidence has confirmed that elective nodal irradiation or surgical disruption of nodal areas can significantly diminish the local and systemic anti-tumor responses stimulated by radio-immunotherapy.<sup>20,21,34,35</sup> Our research provides a clear explanation for this phenomenon. Moreover, it suggests that adopting a neoadjuvant approach to combination therapy, especially in melanoma cases where the draining lymph nodes remain unaffected by surgery or radiation, could lead to enhanced synergy and more potent anti-tumor immune responses. Furthermore, for the induction of an abscopal response at metastatic sites, it is crucial that these sites have effective nodal drainage to efficiently trigger an immune response. Future research will explore strategies to circumvent the reliance on the TdLN. As previously mentioned, numerous clinical

scenarios involve tumors that either lack strong nodal drainage or present challenges in assessing such drainage. Consequently, if it's possible to emulate a TdLN-like microenvironment within the tumor itself or other secondary lymphoid organs, this could potentially overcome the anatomical and immunological constraints currently faced.

While IFN-I is known to foster effector differentiation<sup>38</sup>, its precise role in the differentiation of stem-like T cells within the TdLN remains uncharted. We have demonstrated that the differentiating stem-effector subset expresses a significant level of IFN-I stimulated genes, indicating a pivotal role in stem-like differentiation. To ascertain whether IFN-I signaling is essential for this differentiation process, our ongoing investigations are employing IFNAR1 knockout murine models. These models are instrumental in unraveling the complex synergies between RT and anti-PD-L1 treatment. Through this research, we aim to deepen our comprehension of the dynamic interactions among radiation therapy, immune checkpoint inhibition, and the immune system's anticancer response. By elucidating the underlying molecular pathways and immune mechanisms, we aim to enhance the anticancer efficacy of combination therapies. Such breakthroughs will not only enrich our basic knowledge of cancer immunology but will also facilitate the creation of more potent cancer treatments, offering new hope to patients.

### **Limitations**

In this study, we assessed the critical roles of the TdLN and stem-like T cells in the synergistic effect observed with the combination of radiation therapy (RT) and anti-PD-L1 in murine melanoma models, which mirror numerous facets of human immunology.<sup>25</sup> However, to establish the relevance of these findings to human disease, data derived from human studies are imperative. Clinical trials aimed at evaluating the immunological impact of neoadjuvant RT combined with anti-PD-1/L1 in melanoma are in the planning stages. Furthermore, since our investigations were confined to melanoma, it is necessary to explore other cancer types in the future to establish the generalizability of our findings. Lastly, while our study sheds light on the importance of RT in promoting stem-like T cell differentiation, the precise mechanism underlying this process remains to be fully elucidated and will be the focus of future investigations.

## **Methods**

### **Murine Models**

Female C57BL/6 mice, aged six weeks, were acquired from the Jackson Laboratory, adhering strictly to the ethical guidelines set forth by the Emory University Institutional Animal Care and Use Committee. Euthanasia was carried out for any mice exhibiting signs of illness, lethargy, or experiencing a weight loss exceeding 10% before reaching the predetermined tumor volume endpoint. The melanoma cell line B16F10, acquired from the American Type Culture Collection (ATCC), was modified to express the glycoprotein (GP) of the LCMV Armstrong strain through lentiviral transduction, a method previously outlined.<sup>21</sup> In brief, the process involved cloning the codon-optimized GP into a bicistronic, replication-deficient lentiviral vector (pLVX-IRES-ZsGreen1, Takara), subsequently generating lentiviral particles in 293 T cells (ATCC), and introducing the lentivirus into B16F10 cells. The resultant B16F10GP cell line, expressing high levels of green fluorescent protein ZsGreen1, was refined using a FACS AriaII sorter (BD Biosciences) two weeks post-transduction. Cultivation of the cell line occurred in Dulbecco's Modified Eagle Medium (DMEM), enriched with 10% fetal bovine serum (FBS), 100 units/mL penicillin, 100 µg/mL streptomycin, and 2 mM glutamine, under conditions of 37°C and 5% CO<sub>2</sub>.

### **Tumor Irradiation**

An initial injection of  $5 \times 10^5$  B16F10GP cells was administered subcutaneously into the right flank of the mice on day 0, followed by a similar injection into the left flank on day 3. Upon palpable tumor development, typically between 10 to 12 days post-injection, the right-sided tumors were subjected to irradiation employing the Small Animal Radiation Therapy (SmART+) apparatus by Precision. Throughout the irradiation process, mice were sedated using a system delivering isoflurane anesthesia. A singular dose of 10 Gy radiation was applied. The irradiation protocol was designed using the SmART ATP – Advanced Treatment Planning software. Tumor dimensions were regularly measured with calipers, and the tumor volume was computed using the formula:  $\text{volume} = (\text{length} \times \text{width} \times \text{depth}) \times 0.52$ . In the context of the FTY720 study, the compound was dissolved in the drinking water at a concentration of 2 µg/mL 2 days preceding the radiation therapy and maintained for the duration of the experiment. The αPD-L1 immunotherapy was administered intraperitoneally at a concentration of 200 µg per mouse. For the purpose of T cell analysis, mice were euthanized on the 19th day post-injection, facilitating the collection of tumor tissue, spleen, blood, and TdLN specimens.

### **Adoptive T cell transfer**

Splenocytes designated as P14 cells were harvested from P14 mice. Subsequently, B6 recipient mice, characterized by the CD45.1 phenotype, received a retro-orbital injection of  $2.5 \times 10^5$  P14 cells, administered one day before the introduction of B16F10GP tumor cells.

### **Flow Cytometry**

Flow cytometry assays were conducted utilizing a BD FACSymphony A3 instrument. Procedures for direct ex vivo and intracellular cytokine staining utilized fluorochrome-labeled antibodies, as previously detailed.<sup>21</sup> Identification of tumor-specific CD8<sup>+</sup> T cells was achieved through the preparation of MHC-I tetramers, following established protocols.<sup>21</sup> For the intracellular assessment of transcription factors, including T-cell factor-1 (Tcf-1), cells underwent surface staining for 30 minutes, followed by fixation and permeabilization with the Foxp3 Fixation/Permeabilization Kit (eBioscience), in line with the manufacturer's guidelines. Subsequent intracellular staining was conducted for an additional 30 minutes. These staining processes were uniformly executed in 96-well plates, employing splenocytes as single-color controls. Data acquired from fluorescence-activated cell sorting (FACS) were analyzed using the FlowJo software, version 10.8.

### **Cell Sorting**

For single-cell RNA sequencing, CD8<sup>+</sup> PD-1<sup>+</sup> CD44<sup>+</sup> cells isolated from TdLNs were sorted using a FACSAria (BD) flow cytometry system. Each mouse's samples were uniquely coded using a hashing technique (BioLegend) before being pooled for sequencing analysis. Stem-like P14 cells for adoptive transfer were selected by sorting a subset of CD8<sup>+</sup> PD-1<sup>+</sup> CD44<sup>+</sup> Tim3<sup>-</sup> cells from the TdLNs using the FACSAria (BD) flow cytometry system.

### **Single-cell RNA Sequencing**

Single-cell RNA sequencing was carried out using the 10x Genomics Chromium Controller, with data preprocessing via the Cell Ranger Suite (version 5.0.1) for de-multiplexing and gene counting, aligning against the mm10–2020 mouse genome. Analysis was conducted in R (version 4.2.1), utilizing Seurat (version 4.1.1) for cell deconvolution and normalization, with cells from TdLN specifically targeted. Quality control excluded cells with high mitochondrial content or low gene expression, resulting in 38,578 cells retained across various treatment groups for subsequent analyses. Data normalization and variable gene identification were performed using Seurat, with Uniform Manifold Approximation and Projection (UMAP) for data

visualization.<sup>36</sup> Cell clusters were annotated based on existing datasets<sup>22,29</sup> or differential gene expression analysis, and cellular trajectories were established using Monocle 3, focusing on cells with high *Tcf7* expression to trace differentiation pathways.<sup>37</sup>

### **Statistical Analysis**

Data from all experiments underwent analysis via Prism 9 (GraphPad Software), with summary graphs displaying means  $\pm$  SEM. Statistical significance across experiments was assessed using one-way analysis of variance (ANOVA), or according to specifications in the figure legends. A P value threshold of  $<0.05$  was established for denoting statistical significance (\*).

## **References**

1. Hashimoto, M., Kamphorst, A. O., Im, S. J., et al. (2018). CD8 T cell exhaustion in chronic infection and cancer: Opportunities for interventions. *Annual Review of Medicine*, *69*, 301–318.
2. McLane, L. M., Abdel-Hakeem, M. S., & Wherry, E. J. (2019). CD8 T cell exhaustion during chronic viral infection and cancer. *Annual Review of Immunology*, *37*, 457–495.
3. Abdel-Hakeem, M. S., Manne, S., Beltra, J. C., et al. (2021). Epigenetic scarring of exhausted T cells hinders memory differentiation upon eliminating chronic antigenic stimulation. *Nature Immunology*, *22*(8), 1008–1019.
4. Johnson, P. C., Gainor, J. F., Sullivan, R. J., Longo, D. L., & Chabner, B. (2023). Immune checkpoint inhibitors - The need for innovation. *New England Journal of Medicine*, *388*(16), 1529–1532.
5. Freeman, G. J., Long, A. J., Iwai, Y., et al. (2000). Engagement of the PD-1 immunoinhibitory receptor by a novel B7 family member leads to negative regulation of lymphocyte activation. *Journal of Experimental Medicine*, *192*(7), 1027–34.
6. Huang, A. C., Postow, M. A., Orlowski, R. J., et al. (2017). T-cell invigoration to tumour burden ratio associated with anti-PD-1 response. *Nature*, *545*(7652), 60–65.
7. Barber, D. L., Wherry, E. J., Masopust, D., et al. (2006). Restoring function in exhausted CD8 T cells during chronic viral infection. *Nature*, *439*(7077), 682–7.
8. Eberhardt, C. S., Kissick, H. T., Patel, M. R., et al. (2021). Functional HPV-specific PD-1(+) stem-like CD8 T cells in head and neck cancer. *Nature*, *597*(7875), 279–284.
9. Sade-Feldman, M., Yizhak, K., Bjorgaard, S. L., et al. (2019). Defining T cell states associated with response to checkpoint immunotherapy in melanoma. *Cell*, *176*(1–2), 404.
10. Siddiqui, I., Schaeuble, K., Chennupati, V., et al. (2019). Intratumoral Tcf1(+)PD-1(+)CD8(+) T cells with stem-like properties promote tumor control in response to vaccination and checkpoint blockade immunotherapy. *Immunity*, *50*(1), 195–211 e10.
11. Im, S. J., Hashimoto, M., Gerner, M. Y., et al. (2016). Defining CD8+ T cells that provide the proliferative burst after PD-1 therapy. *Nature*, *537*(7620), 417–421.
12. Abuodeh, Y., Venkat, P., & Kim, S. (2016). Systematic review of case reports on the abscopal effect. *Current Problems in Cancer*, *40*(1), 25–37.
13. Wersäll, P. J., Blomgren, H., Pisa, P., Lax, I., Kalkner, K. M., & Svedman, C. (2006). Regression of non-irradiated metastases after extracranial stereotactic radiotherapy in metastatic renal cell carcinoma. *Acta Oncologica*, *45*(4), 493–497.
14. Kingsley, D. P. (1975). An interesting case of possible abscopal effect in malignant melanoma. *British Journal of Radiology*, *48*(574), 863–866.

15. Theelen, W., Peulen, H. M. U., Lalezari, F., et al. (2019). Effect of Pembrolizumab after stereotactic body radiotherapy vs Pembrolizumab alone on tumor response in patients with advanced non-small cell lung cancer: Results of the PEMBRO-RT Phase 2 randomized clinical trial. *JAMA Oncology*.
16. McBride, S., Sherman, E., Tsai, C. J., et al. (2020). Randomized phase II trial of Nivolumab with stereotactic body radiotherapy versus Nivolumab alone in metastatic head and neck squamous cell carcinoma. *Journal of Clinical Oncology*.
17. Twyman-Saint Victor, C., Rech, A. J., Maity, A., et al. (2015). Radiation and dual checkpoint blockade activate non-redundant immune mechanisms in cancer. *Nature*, 520(7547), 373–377.
18. Luke, J. J., Lemons, J. M., Karrison, T. G., et al. (2018). Safety and clinical activity of Pembrolizumab and multisite stereotactic body radiotherapy in patients with advanced solid tumors. *Journal of Clinical Oncology*, 36(16), 1611–1618.
19. Theelen, W., Peulen, H. M. U., Lalezari, F., et al. (2019). Effect of Pembrolizumab after stereotactic body radiotherapy vs Pembrolizumab alone on tumor response in patients with advanced non-small cell lung cancer: Results of the PEMBRO-RT Phase 2 randomized clinical trial. *JAMA Oncology*, 5(9), 1276–1282.
20. Marciscano, A. E., Ghasemzadeh, A., Nirschl, T. R., et al. (2018). Elective nodal irradiation attenuates the combinatorial efficacy of stereotactic radiation therapy and immunotherapy. *Clinical Cancer Research*, 24(20), 5058–5071.
21. Buchwald, Z. S., Nasti, T. H., Lee, J., et al. (2020). Tumor-draining lymph node is important for a robust abscopal effect stimulated by radiotherapy. *Journal of Immunotherapy Cancer*, 8(2).
22. Huang, Q., Wu, X., Wang, Z., et al. (2022). The primordial differentiation of tumor-specific memory CD8(+) T cells as bona fide responders to PD-1/PD-L1 blockade in draining lymph nodes. *Cell*, 185(22), 4049–4066 e25.
23. Chamoto, K., Chowdhury, P. S., Kumar, A., et al. (2017). Mitochondrial activation chemicals synergize with surface receptor PD-1 blockade for T cell-dependent antitumor activity. *Proceedings of the National Academy of Sciences of the United States of America*, 114(5), E761–E770.
24. Francis, D. M., Manspeaker, M. P., Schudel, A., et al. (2020). Blockade of immune checkpoints in lymph nodes through locoregional delivery augments cancer immunotherapy. *Science Translational Medicine*, 12(563).
25. Prokhnevska, N., Cardenas, M. A., Valanparambil, R. M., et al. (2023). CD8(+) T cell activation in cancer comprises an initial activation phase in lymph nodes followed by effector differentiation within the tumor. *Immunity*, 56(1), 107–124 e5.
26. Connolly, K. A., Kuchroo, M., Venkat, A., et al. (2021). A reservoir of stem-like CD8(+) T cells in the tumor-draining lymph node preserves the ongoing antitumor immune response. *Science Immunology*, 6(64), eabg7836.



27. Chen, S., Lee, L. F., Fisher, T. S., et al. (2015). Combination of 4–1BB agonist and PD-1 antagonist promotes antitumor effector/memory CD8 T cells in a poorly immunogenic tumor model. *Cancer Immunology Research*, 3(2), 149–160.
28. Kleffel, S., Posch, C., Barthel, S. R., et al. (2015). Melanoma cell-intrinsic PD-1 receptor functions promote tumor growth. *Cell*, 162(6), 1242–1256.
29. Miller, B. C., Sen, D. R., Al Abosy, R., et al. (2019). Subsets of exhausted CD8(+) T cells differentially mediate tumor control and respond to checkpoint blockade. *Nature Immunology*, 20(3), 326–336.
30. Janopaul-Naylor, J. R., Shen, Y., Qian, D. C., & Buchwald, Z. S. (2021). The Abscopal Effect: A Review of Pre-Clinical and Clinical Advances. *International Journal of Molecular Sciences*, 22(20).
31. Boukhaled, G. M., Harding, S., & Brooks, D. G. (2021). Opposing roles of type I interferons in cancer immunity. *Annual Review of Pathology*, 16, 167–198.
32. McBride, S., Sherman, E., Tsai, C. J., et al. (2021). Randomized phase II trial of Nivolumab with stereotactic body radiotherapy versus Nivolumab alone in metastatic head and neck squamous cell carcinoma. *Journal of Clinical Oncology*, 39(1), 30–37.
33. Lee, N. Y., Ferris, R. L., Psyrri, A., et al. (2021). Avelumab plus standard-of-care chemoradiotherapy versus chemoradiotherapy alone in patients with locally advanced squamous cell carcinoma of the head and neck: a randomised, double-blind, placebo-controlled, multicentre, phase 3 trial. *Lancet Oncology*, 22(4), 450–462.
34. Saddawi-Konefka, R., O’Farrell, A., Faraji, F., et al. (2022). Lymphatic-preserving treatment sequencing with immune checkpoint inhibition unleashes cDC1-dependent antitumor immunity in HNSCC. *Nature Communications*, 13(1), 4298.
35. Darragh, L. B., Gadwa, J., Pham, T. T., et al. (2022). Elective nodal irradiation mitigates local and systemic immunity generated by combination radiation and immunotherapy in head and neck tumors. *Nature Communications*, 13(1), 7015.
36. Becht, E., McInnes, L., Healy, J., et al. (2018). Dimensionality reduction for visualizing single-cell data using UMAP. *Nature Biotechnology*.
37. Cao, J., Spielmann, M., Qiu, X., et al. (2019). The single-cell transcriptional landscape of mammalian organogenesis. *Nature*, 566(7745), 496–502.
38. Jergovic, M., Coplen, C. P., Uhrlaub, J. L., et al. (2021). Infection-induced type I interferons critically modulate the homeostasis and function of CD8(+) naive T cells. *Nature Communications*, 12(1), 5303.

Supporting Figures for:

**Synergistic Paradigm of Radiotherapy and PD-L1 Blockade Orchestrates the Induction of Stem-Like T Cell Populations within the Tumor-Draining Lymph Node**

By

Patan Tippitak

Zachary S. Buchwald MD PhD

Adviser

**Supporting Figures**

- Figure S1.* RT combined with anti-PD-L1 enhances tumor suppression and boosts the presence of IFN $\gamma$ <sup>+</sup> CD8<sup>+</sup> T cells within the tumor 21
- Figure S2.* FTY720 treatment negated the increase in Gp33<sup>+</sup> T cells and weakened the tumor growth control achieved by RT or anti-PD-L1 22
- Figure S3.* FTY720 administration elevated the presence of Gp33<sup>+</sup> T cells and the quantity of stem-like T cells in the TdLN 23
- Figure S4.* RT and anti-PD-L1 therapy together enhance the proliferation and differentiation of stem-like T cells 24

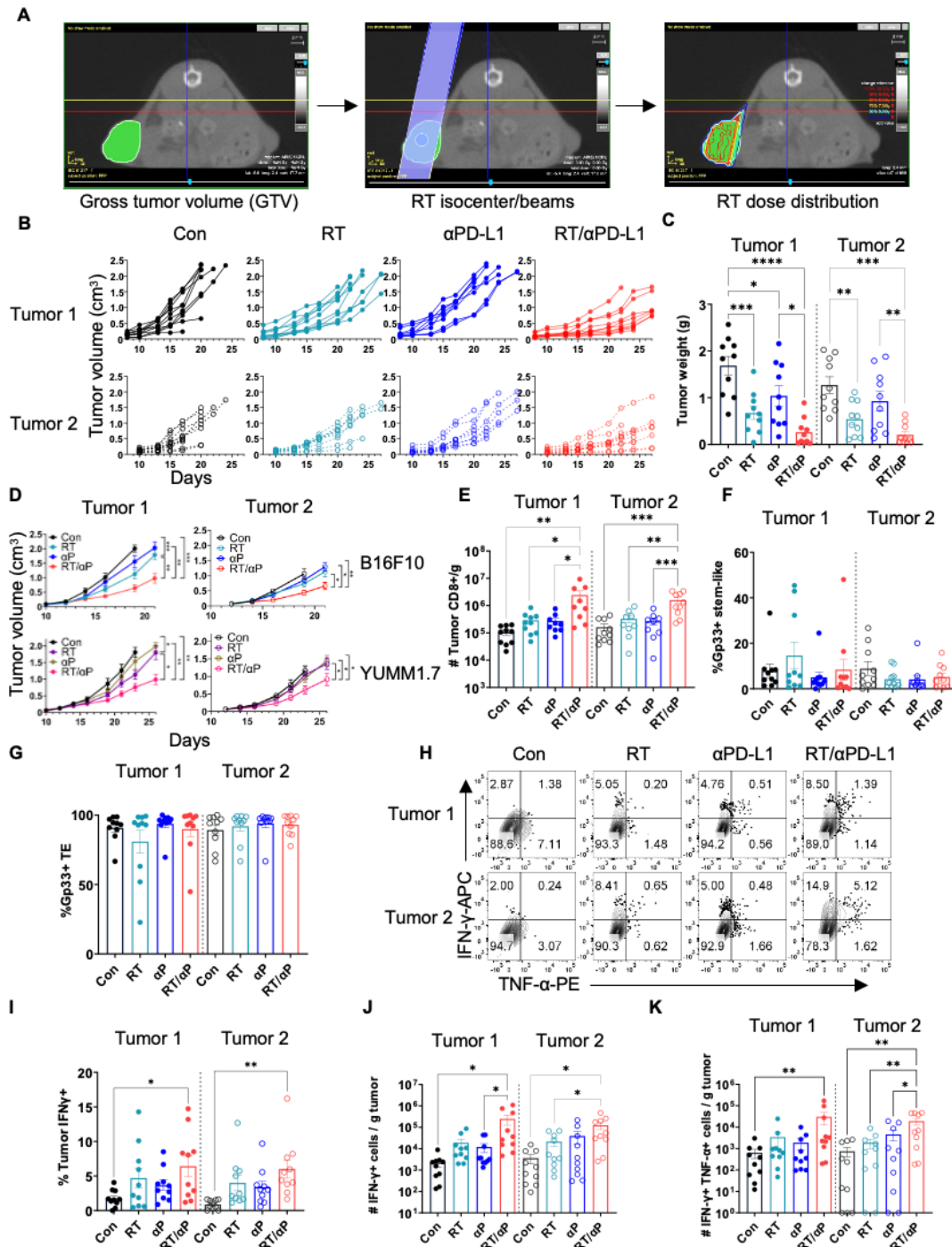


**Figure S1. RT combined with anti-PD-L1 enhances tumor suppression and boosts the presence of IFN $\gamma$ + CD8+ T cells within the tumor.** (A) Tumor visualization: GTV, RT center, beams, dose, and isodose lines. (B) B16F10GP tumor growth under various treatments. (C) Tumor weights by treatment. (D) Growth kinetics for B16F10 parental and Yumm1.7 tumors under varying treatments. (E) CD8+ T cell quantification per tumor gram. (F) Stem-like cell frequency in tumors. (G) TE frequency in tumors. (H) IFN- $\gamma$ + TNF- $\alpha$ + cell flow plots in tumors. (I) IFN- $\gamma$ + cell frequency in tumors. (J) IFN- $\gamma$ + cell count per tumor gram. (K) TNF- $\alpha$ + IFN- $\gamma$ + T cell quantification per tumor gram. \*Significance levels: \* $p < 0.05$ , \*\* $p < 0.01$ , \*\*\* $p < 0.001$ , \*\*\*\* $p < 0.0001$  (ANOVA). Combined data from 2 experiments (n=10).

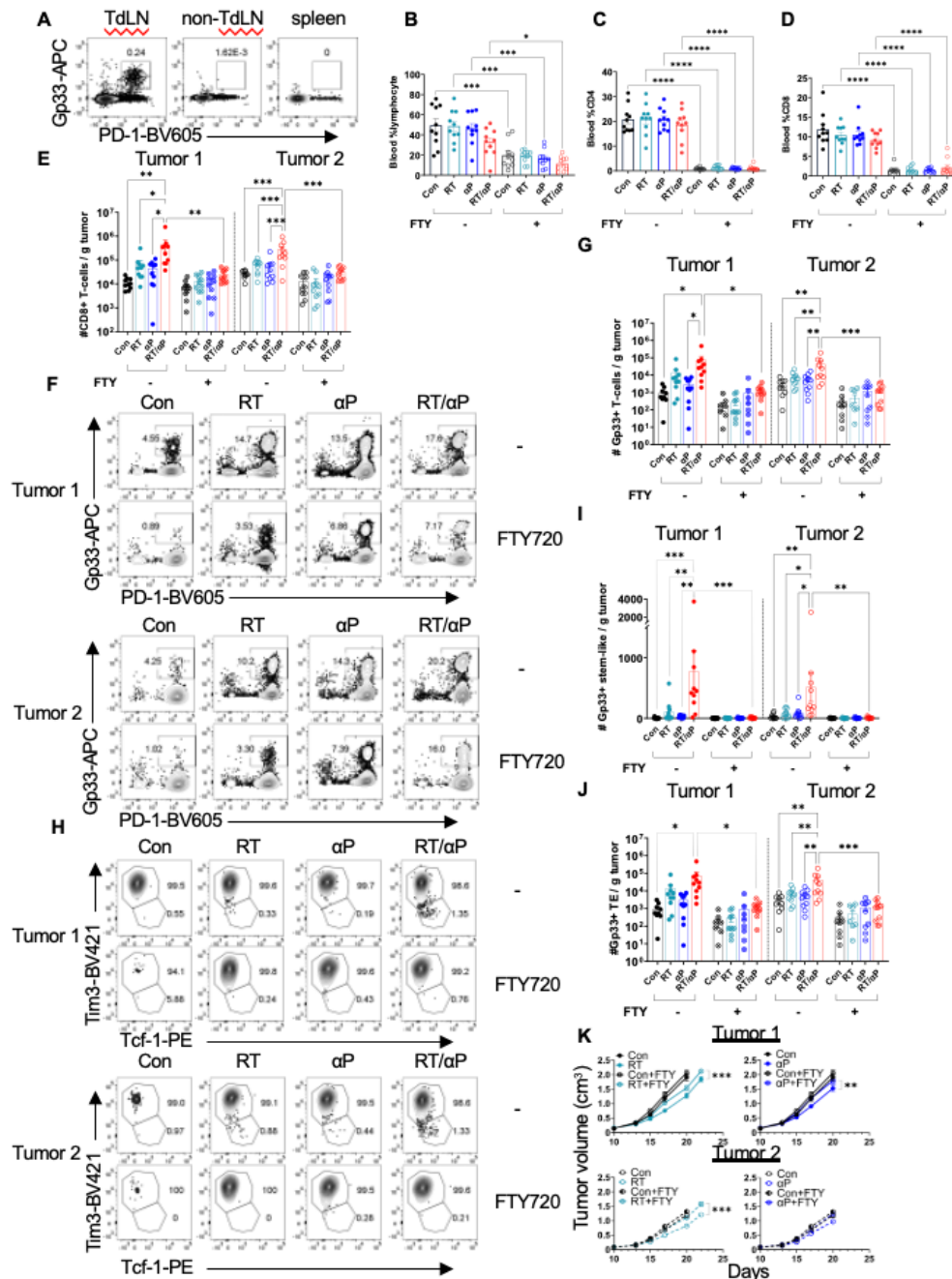


**Figure S2. FTY720 treatment negated the increase in Gp33+ T cells and weakened the tumor growth control achieved by RT or anti-PD-L1.** (A) Gp33+ T cell flow plots in lymphoid tissues. (B) Lymphocyte frequencies in blood. (C) Blood CD4+ T cell frequencies. (D) Blood CD8+ T cell frequencies. (E) CD8+ T cell quantification per tumor gram. (F) Gp33+ T cells in tumors, with/without FTY720, flow plots. (G) Quantification of Gp33+ T cells in tumors, treatments with/without FTY720. (H) Flow plots of Gp33+ stem-like/TE T cells in tumors, treatments with/without FTY720. (I) Quantification of Gp33+ stem-like T cells per tumor gram. (J) TE quantification per tumor gram. Data from 2 experiments combined (n=10). (K) Tumor growth under various treatments, with/without FTY720. N=15 from 2 experiments. \*Significance level: \*p<0.05, \*\*p<0.01, \*\*\*p<0.001, \*\*\*\*p<0.0001 (ANOVA).

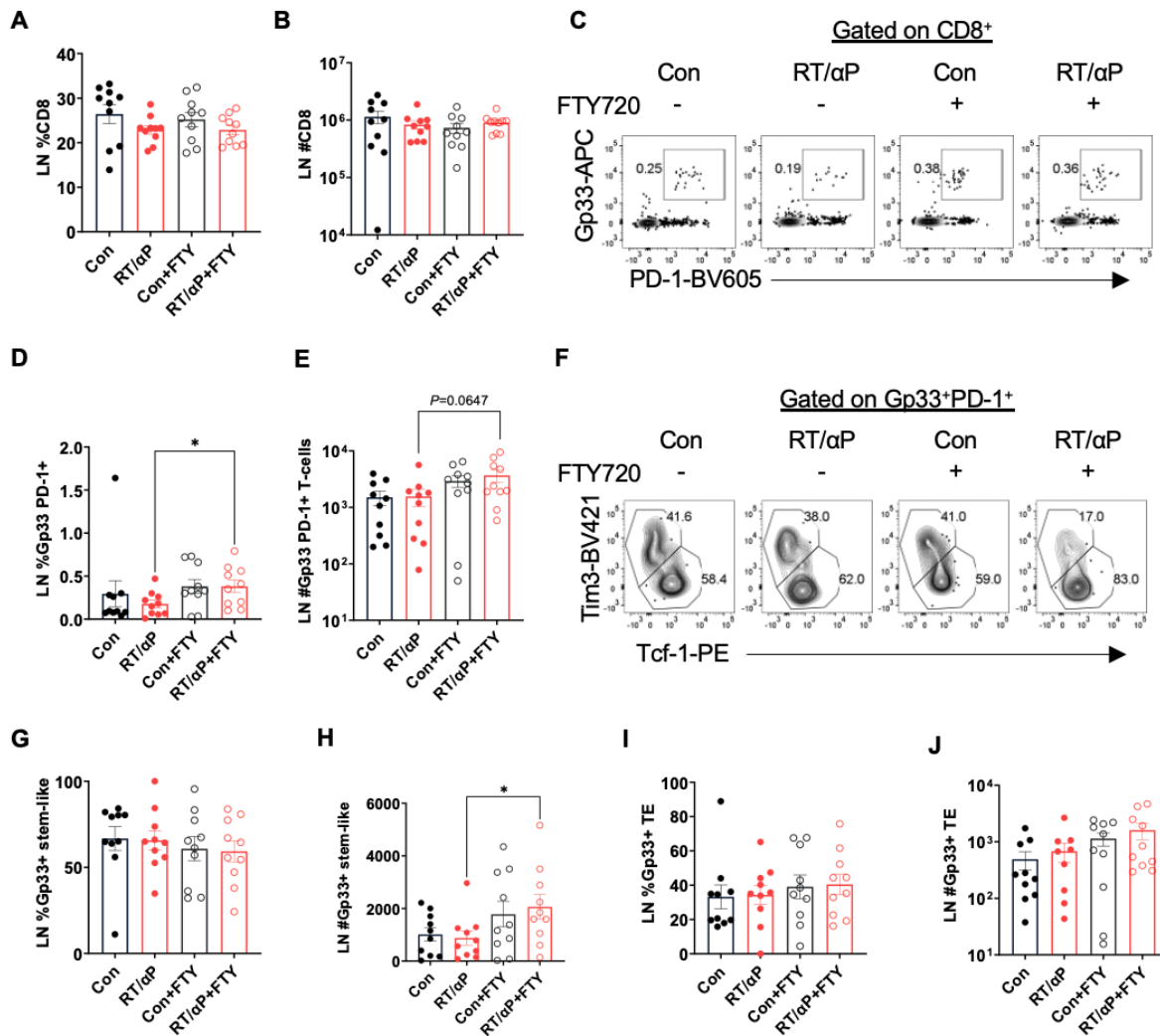


**Figure S3. FTY720 administration elevated the presence of Gp33<sup>+</sup> T cells and the quantity of stem-like T cells in the TdLN.** (A) CD8<sup>+</sup> T cell frequency in TdLN, with/without FTY720 treatment. (B) CD8<sup>+</sup> T cell count in TdLN, with/without FTY720 treatment. (C) Gp33<sup>+</sup> T cells in TdLN, flow plots, with/without FTY720 treatment. (D) Gp33<sup>+</sup> T cell frequency in TdLN, with/without FTY720. (E) Gp33<sup>+</sup> T cell count in TdLN, with/without FTY720. (F) Gp33<sup>+</sup> stem-like/TE T cells in TdLN, flow plots, with/without FTY720. (G) Frequency of Gp33<sup>+</sup> stem-like T cells in TdLN, with/without FTY720. (H) Count of Gp33<sup>+</sup> stem-like T cells in TdLN, with/without FTY720. (I) Frequency of TE in TdLN, with/without FTY720. (J) Count of TE in TdLN, with/without FTY720. N=10 mice per group. \*Significance level: \* $p < 0.05$  (two-tailed t-test).

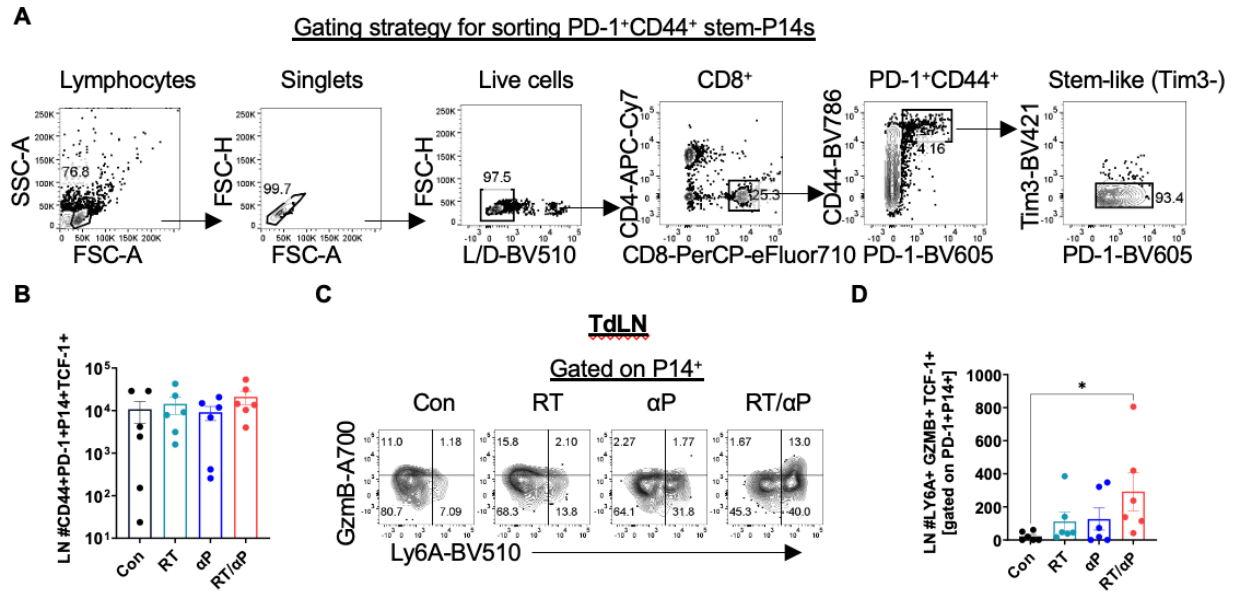


**Figure S4. RT and anti-PD-L1 therapy together enhance the proliferation and differentiation of stem-like T cells.** (A) Strategy for isolating PD-1<sup>+</sup> CD44<sup>+</sup> stem-P14s via gating. (B) Quantification of CD44<sup>+</sup> PD-1<sup>+</sup> P14<sup>+</sup> Tcf-1<sup>+</sup> cells in TdLN. (C) Flow plots of Ly6a<sup>+</sup> GzmB<sup>+</sup> cells in TdLN. (D) Quantification of Ly6a<sup>+</sup> GzmB<sup>+</sup> Tcf-1<sup>+</sup> cells in TdLN.